IUST
Iran University of Science and Technology

Iranian Journal of Electrical and Electronic Engineering

Journal Homepage: ijeee.iust.ac.ir

Research Paper

Modified Impedance-Based OOS Protection Based on On-Line Thévenin Equivalent Estimation

S. R. Hosseini*, M. Karrari*(C.A.), and H. Askarian Abyaneh*

Abstract: In this paper, a novel approach based on the Thévenin tracing is presented to modified conventional impedance-based out-of-step (OOS) protection. In conventional approach, the OOS detection is done by measuring positive sequence impedance. However, the measured impedance may be change due to different factors such as capacitor bank switching and reactive power compensators that it can cause the relay to malfunction. In this paper, first, an on-line Thévenin equivalent (TE) approach based on the recursive least square (RLS) is presented. Then, a protection function is developed based on online network Thévenin equivalent parameters to correct the measured impedance path. The main feature of this method is the use of local voltage and current measurements for Thévenin equivalent estimation and OOS protection. The performance of the proposed method is investigated by simulation of synchronous generator OOS protection function in the presence of a static synchronous compensator (STATCOM). The simulation results show that, STATCOM changes the impedance path and can cause the incorrect diagnosis of OOS relay. Furthermore, the proposed method corrects the impedance path and improves the accuracy of OOS impedance-based function when the STATCOM is installed in system.

Keywords: Thévenin Equivalent, STATCOM, Out-of-Step Protection, Synchronous Generator.

1 Introduction

UNDER normal power system conditions, the generators synchronously work together. When a sever disturbance (such as faults and switching near the generators) occurs in the network, the electrical power fluctuates and causes to oscillation of the rotor angles. Under unstable power swing condition, the rotor angle crosses from critical angle and the synchronism is lost [1]. Out of step (OOS) is another name that refers to this condition. The OOS of a generator not only is a threat for its mechanical components, but also may affect the stability of the other generators in the network. In this condition, the unstable generator should be quickly disconnected from system to prevent damage to unstable generator and helps to save the rest of the system from total instability [2-4].

Conventional method for OOS detection is impedance-based approach that detects OOS by comparing positive sequence impedance trajectory with predetermined characteristic at the R-X plane [2-6]. The settings of characteristic are obtained based on numerous contingency simulation studies. However, these settings are not compatible and should be modified by change of the power system parameters. Many new techniques have been proposed to detect the OOS condition in the literatures. Equal area criterion, extended equal area criterion, swing center voltage, and distributed dynamic state estimator are some of these approaches that are compatibility and strength against changes in power system configuration [7-12]. However, these approaches are complicated, difficult to implement and need at least the instance of fault clearing time to be fed as an input to the relay [2]. Therefore, the impedance-based techniques are still incorporated for OOS condition detection.

In addition to power system changes, the presence of

Iranian Journal of Electrical and Electronic Engineering, 2021.
Paper first received 01 November 2019, revised 20 March 2020, and accepted 07 April 2020.
* The authors are with the Depatrment of Electrical Engineering, Amirkabir University of Technology, Tehran, Iran.
E-mails: sr.hosseini@aut.ac.ir, karrari@aut.ac.ir, and askarian@aut.ac.ir.
Corresponding Author: M. Karrari.
https://doi.org/10.22068/IJEEE.17.1.1690

FACTS devices can also affect impedance-based protections. The effect of FACTS devices on distance [13-23] and loss-of-excitation (LOE) protection [24-27] have investigated in the literatures. Results show that the presence of various series and shunt controllers usually makes distance relays under-reach, thereby changing trip characteristic of the distance relay [15]. Also, results revealed that the presence of FACTS causes a substantial delay in the performance of LOE relay.

The performance of distance relays for power swing detection have evaluated in [28-32]. These studies have been done in the presence of various reactive power compensators such as fix capacitor [28, 29], SSSC [30] and UPFC [31, 32].

The impacts of UPFC and STATCOM on the performance of OOS protection were investigated by authors in [33-34] and a novel modification function has been presented. The results of [34] indicate the OOS may be not detected in the presence of STATCOM. To solve this problem, an analytical adaptive approach was proposed to eliminate the effect of STATCOM. The proposed approach resolved the problem, but it required sending remote bus voltage and current phasors to the relay location. Following on from previous work, the authors have attempted to eliminate this requirement by presenting a new approach.

In this study, a protection function is developed based on online network Thévenin equivalent (TE) parameters to correct the measured impedance path. The main feature of this method is the use of local voltage and current measurements for TE estimation and OOS protection. In the proposed approach, the TE estimation is done by recursive least square (RLS) technique applies to the time variant system identification. Contributions of this paper are as follows:

1. On-line TE estimation of network is done by RLS technique based on time variant system identification theories.
2. An adaptive method based on online estimation of network Thévenin parameters are presented to resolved remote bus data requirement for proposed approach in [34].

2 Synchronous Generator OOS Condition

For a generator connected to power network as shown in Fig. 1, the relationship between rotor angle and transitional Power is defined through known equations (1) and (2) as follow:

$$\frac{d^2\delta}{dt^2} = \frac{\omega_s}{2H}(P_m - P_e) - \frac{D}{2H}\frac{d\delta}{dt} \quad (1)$$

$$P_e = \frac{E_A E_B}{Z_{tot}}\sin\delta \quad (2)$$

where, δ, P_m, P_e, and ω_s are rotor angle, mechanical power, electrical power and base synchronous speed, respectively. E_A is magnitude of generator internal voltage and E_B is the magnitude of external system voltage. The phase difference between these two phasors is equal to the rotor angle.

Following disturbances in power system, the electrical power oscillates and according to (1) the rotor angle also swings. As shown in Fig. 2, by increasing δ, electrical centre voltage (V_{EC}) decreases. In the power system shown in Fig. 1, the electrical center is a point that the impedance between each voltage source and this point is equal. When the rotor angle reaches 180 degrees, V_{EC} is exactly zero in all three phases. In this condition, if the electrical center is within the transmission line, this point would be viewed by the transmission line relays as a three-phase fault and the relays would pick up to clearing the line.

With addition of transmission lines, the power system becomes stronger and the impedance of system decreases. In this condition, the electrical center tends to occur within the generator or its corresponding step-up transformer. In this situation a special relay must be provided at the generator. Such a situation occurs when a generator pulls out of synchronism in a system with strong transmission. A low excitation level on the generator ($E_A < E_B$) also tends to contribute to such condition. Therefore, the OOS protection is necessary to detect and initiate appropriate control action to avoid adverse effects on the affected generator and the rest of the system [2].

One of the most commonly used to power swing protection, is based on impedance measurement at the generator terminal. The measured impedance is related to the rotor angle according to (3) [2]. In this

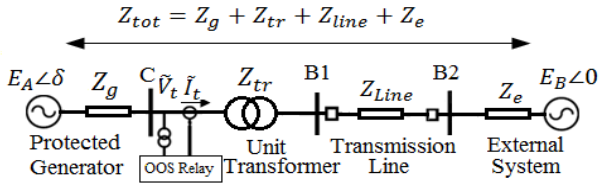

Fig. 1 Single-machine infinite bus system.

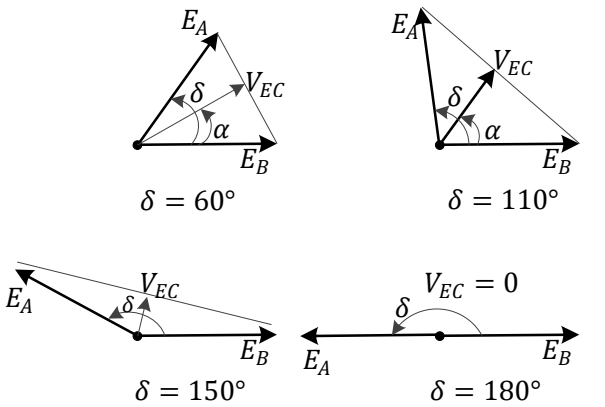

Fig. 2 The voltage of electrical centre with increasing the rotor angle.

equation, Z_R, Z_g, and Z_{tot} are measured impedance, generator impedance and total impedance between E_A and E_B, respectively.

$$Z_R = -Z_g - \frac{Z_{tot}}{1-\frac{1}{K}e^{-j\delta}} \quad \& \quad K = \frac{E_A}{E_B} \tag{3}$$

There are several methods, such as single-blinder, double blinder, concentric schemes, swing centre voltage, equal area criteria based and etc. to OOS protection [2-12]. This study is the continuation of previous authors' study about the effect of STATCOM on the impedance-based OOS protection [34]. The single blinder scheme is used in the current study that the principle of this scheme with detail of characteristic was discussed in [35]. The characteristic of this scheme is shown in Fig. 3.

3 The Measured Impedance in the Presence of STATCOM

In [34] the performance of STATCOM on the impedance-based OOS protection was investigated by authors and a novel modification function has been presented. The results of [34] indicate the OOS may be not detected in the presence of STATCOM. To solve this problem, an analytical adaptive approach was proposed to eliminate the effect of STATCOM. The proposed approach resolved the problem, but it required sending remote bus voltage and current phasors to the relay location. In this study, authors have attempted to eliminate this requirement by presenting a new approach.

Fig. 4(a) illustrates the simplified single-line diagram of the power system introduced in Fig. 1 which a shunt STATCOM is connected to the system at the beginning of the transmission line. This system consists of a synchronous generator connected to an infinite bus by the transmission line. Z_1 is equal to Z_g, Z_{tr} is step up transformer impedance and Z_2 is equal to the transmission line impedance. The equivalent circuit of the right side of B2 busbar can be considered as Thévenin equivalent circuit (see Fig. 4(b)).

Before the installation of STATCOM, the measured impedance by OOS relay obtain by (4) as follow [34]:

$$Z_R = \frac{\tilde{V}_R}{\tilde{I}_R} = \frac{\tilde{E}_1(Z_2+Z_{tr})+\tilde{E}_2 Z_1}{\tilde{E}_1-\tilde{E}_2} \tag{4}$$

In this equation, $\tilde{E}_1$ and $\tilde{E}_2$ represent the generator internal voltage and remote bus voltage phasors, respectively. The phasors $\tilde{V}_R$ and $\tilde{I}_R$ are the voltage and current measured at the generator terminal bus.

According to the equivalent circuit shown in Fig. 4(b), after installing a shunt STATCOM the measured impedance by OOS relay, is obtained by (5) to (7). The extraction process of these equations is discussed in [34].

$$Z_R = \frac{\tilde{V}_R}{\tilde{I}_R} = \frac{\tilde{E}_1(Z_{th})+\tilde{E}_{th} Z_1}{\tilde{E}_1-\tilde{E}_{th}} \tag{5}$$

$$Z_{th} = Z_{tr} + Z_2 \| Y_{sh} = \frac{Z_2}{1+Z_2 Y_{sh}} \quad \& \quad Y_{sh} = \frac{\tilde{I}_{sh}}{\tilde{V}_{B2}} \tag{6}$$

$$\tilde{E}_{th} = \frac{1}{1+Z_2 Y_{sh}} \tilde{E}_2 \tag{7}$$

In these equations, Y_{sh}, $\tilde{V}_{B2}$, $\tilde{I}_{sh}$ are the equivalent admittance, voltage and current of the STATCOM, respectively.

4 Modified Adaptive OOS Protection Based on Thévenin Voltage

Thévenin's theorem is one of the network theorem that

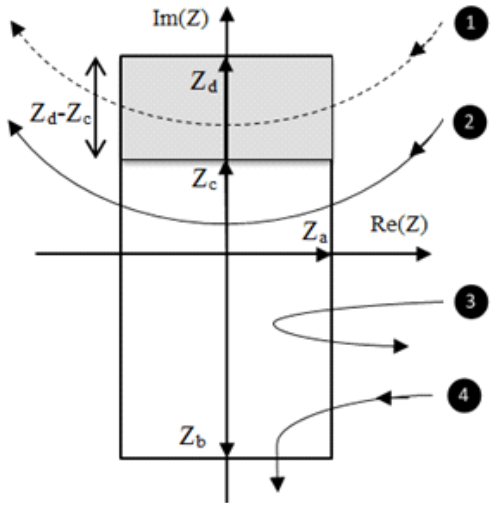

Fig. 3 The characteristic of 7um62 OOS function presented in [35].

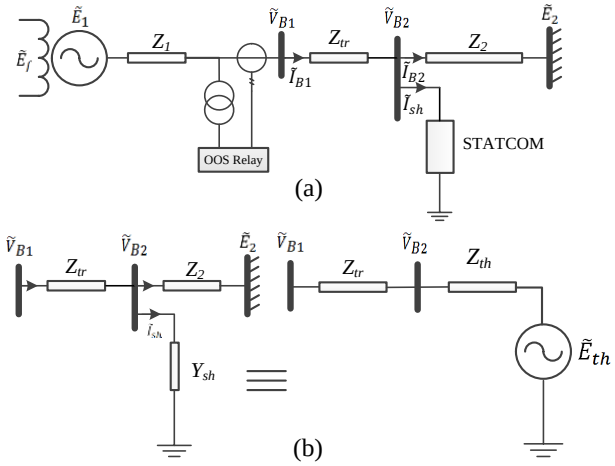

Fig. 4 a) The STATCOM embedded single machine connected infinite bus test system and b) Equivalent network after installing STATCOM.

is valid in linear networks. The concept of TE circuit is simply shown in Fig. 5. According to this theorem, the network in Fig. 5(a) can be replaced by a voltage source in series with impedance as Fig. 5(b).

By comparing the measured impedance with and without STATCOM in equations (4) and (5), it can be concluded that $Z_2 + Z_{tr}$ and $\tilde{E}_2$ in (4) have been replaced with Z_{th} and $\tilde{E}_{th}$ in (5), respectively.

A simple way to eliminate the effect of STATCOM on the impedance path is to ignore Y_{sh} in Fig. 4(b). For this purpose, it is sufficient to use Z_2^{new} instead of Z_{th} in (5). The modified impedance by this method is obtained by (8) as follows:

$$Z_R^{\text{modified}} = \frac{\tilde{E}_1(Z_2^{new}) + \tilde{E}_{th}^{e} Z_1}{\tilde{E}_1 - \tilde{E}_{th}^{e}} \tag{8}$$

where, $\tilde{E}_{th}^{e}$ and Z_R^{modified} are the estimated Thévenin voltage and the modified impedance, respectively. Z_2^{new} is the network side Thévenin impedance without considering the STATCOM. In addition to ignoring STATCOM, the new value of system side impedance must be calculated taking into account the disconnected lines after clearing the fault. It should be noted; that the Thévenin voltage $\tilde{E}_{th}$ must be maintained at its own value. This ensures proper operation of the relay in the stable power swing condition. Finally, the internal voltage $\tilde{E}_1$ in (8) can be calculated using KVL at generator terminal [34].

The system Thévenin voltage changes as the network changes. Network changes such as disconnecting or connecting lines, capacitors, reactors, etc. may be occurring at any time. Therefore, the Thévenin voltage should be estimated on-line. The on-line Thévenin equivalent estimation is discussed in next section.

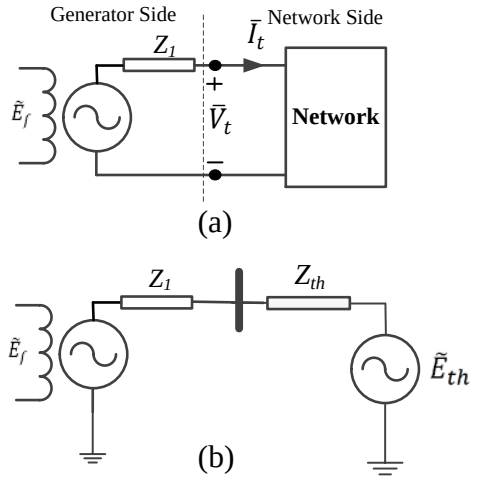

Fig. 5 a) The synchronous generator connected to the network and b) The Thévenin equivalent network

5 On-Line Thévenin Estimation by Recursive Least Square

On-Line identification of systems is done by recursive identification methods. The RLS identification approach is usually used to identify time-variant systems and in this study it is used to determine TE parameters. For this purpose, the network side of the Fig. 5(a) with input $\bar{I}_t$ and output $\bar{V}_t$ considered as identified system. $\bar{V}_t$ and $\bar{I}_t$ are voltage and current phasor samples at any time t, respectively. In all least square based identification approaches a liner equation is defined as linear regression equation. The linear regression equation for TE estimation is defined as (9):

$$y_t = \underline{u}_t^T \underline{\theta} + e_t \; ; \begin{cases} \underline{u}_t^T = \left[1 \bar{I}_t\right] \\ y_t = \bar{V}_t \\ \underline{\theta} = \left[\bar{E}_{th} \; Z_{th}\right]^T \end{cases} \tag{9}$$

where $\tilde{E}_{th}$ and Z_{th} are the unknown parameters of the system.

In RLS estimation, it is assumed that the system have already been identified with N samples of inputs and outputs. By entering a new input-output sample, the identification is done by N+1 samples and the previous estimation is updated based on the new data. The steps of time variable systems identification are as follows [36]:

Step 0: initialize $\underline{\theta}_0$ and P_0.

$\underline{\theta}_0$: The initial value of parameters vector

P_0: The initial value of parameters covariance matrix

A good initial value of $\underline{\theta}_0$ can be found by means of least square approach with a limited number of samples. Moreover, the covariance matrix P_0 initialized as a diagonal matrix according to discussed in [36]. An example of P_0 is given in (10).

$$P_0 = \begin{bmatrix} 100 & 0 \\ 0 & 100 \end{bmatrix} \tag{10}$$

Step 1: receive the new input-output at the time step *t*.
Step 2: create the u_t vector by new input-output.
Step 4: update P_t and k_t by (11) and (12), respectively.

$$P_t = P_{t-1} - \frac{P_{t-1} u_t . u_t^T P_{t-1}}{\lambda + u_t^T P_{t-1} u_t} \tag{11}$$

$$k_t = \frac{P_{t-1} u_t}{1 + u_t^T P_{t-1} u_t} \tag{12}$$

where,

P_t: The covariance matrix of parameter as a $p \times p$ matrix,

k_t : $p \times 1$ vector,

p: the number of unknown parameters,

λ : is a scalar in range 0 and 1 to reduce the effect of older data in estimation [36].

Step5: Calculate the new estimation by (13)

$$\underline{\theta}_t = \underline{\theta}_{t-1} + \frac{1}{\lambda} k_t \left(y_t - u_t^T \hat{\theta}_{t-1} \right) \quad (13)$$

Step 7: go to the next time step (**Step 1**)

For online calculation of TE, at first the initial values $\underline{\theta}_0 = \left[\bar{E}_{th0} \; Z_{th0} \right]^T$ can be adjusted according to the network steady state values. Then, by entering any new samples of $\bar{I}_t$ and $\bar{V}_t$ the $\bar{E}_{th}$ and Z_{th} values are updated based on the above steps.

6 The Performance of Modified OOS Function in the Presence of STATCOM

The effect of STATCOM on the OOS relay function was investigated in [34]. The SMIB test system as shown in Fig. 6 was simulated with ±200 MVA STATCOM to evaluate the OOS performance. Detailed information of the system is given in [34]. The results of mentioned study revealed that the measured impedance trajectory was impacted by STATCOM during out of step condition. The impedance path after a fault at point F with and without STATCOM connected to bus HT is shown in Fig. 7. In the current paper, the same study is done to demonstrate the effectiveness of purposed TE-based approach.

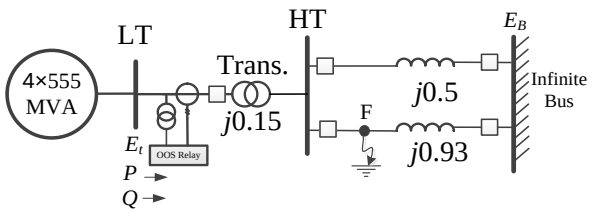

Fig. 6 Single-machine infinite bus system [34].

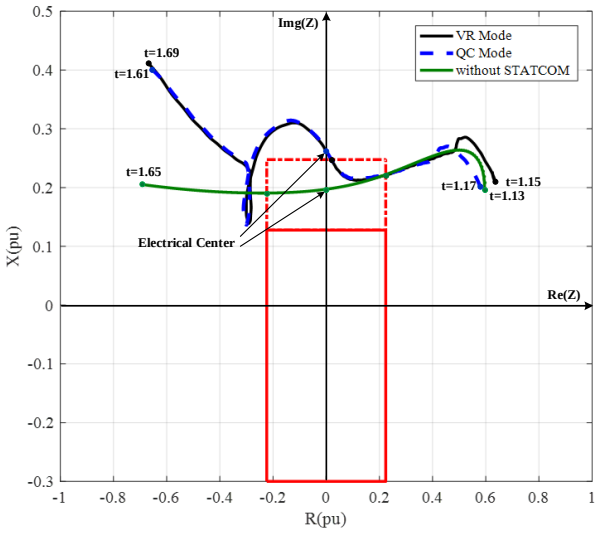

Fig. 7 Impedance trajectory after installing the STATCOM [34].

The fault scenario discussed in [34] has implemented here to compare the results of this study with [34]. A three-phase short circuit fault occurred at the beginning of the second line (Point F) at time t = 1 s, and the second line is disconnected from the network at t = 1.1 s.

6.1 The Thévenin Equivalent Estimation

The Thévenin voltage of network at the generator terminal bus ($\tilde{E}_{th}^{e}$) in (8) estimated as on-line. The performance of TE estimation algorithm presented in section 5 is shown in Figs. 8-14. Three following cases are studied to evaluate the performance of TE estimation. The sampling frequency in the all following studies is equal 25 kHz. Due to the presence of 250 Hz in the frequency components, $f_{sampling}$ = 2.5 kHz is sufficient. But, in the simulation in MATLAB/Simulink environment, due to Ode23 Solver errors, the sampling frequency is considered 25 kHz.

Case 1: Line 2 is disconnected at t = 1.1 s

In this case, the system is in steady state and at the moment t = 1.1s the second line is disconnected. The voltage and current ate the generator terminal bus has been sampled by time step $\Delta t = 10^{-4}$ ms. The initial values of covariance matrix and estimated vector are set as follow:

$$P_0 = \begin{bmatrix} 1000 & 0 \\ 0 & 1000 \end{bmatrix}, \quad \underline{\theta}_0 = \left[0.9008 \; 0.47 \right]^T .$$

The initial value of estimated vector is selected based on steady state value of Thévenin parameters. The forgetting factor λ is set based on adaptive approach discussed in [36]. Fig. 8 shows the Thévenin voltage of network side of generator terminal bus. It is clear that before opening the line 2, $\tilde{E}_{th} = 0.9008$ pu and it does not change after the second line is opened. The variation of the Thévenin impedance is shown in Fig. 9. Before opening the line 2, the Thévenin impedance is equal to 0.47 pu (0.15+0.5||0.93) and after the line is opened, the impedance is changed to 0.65 pu (0.15+0.5).

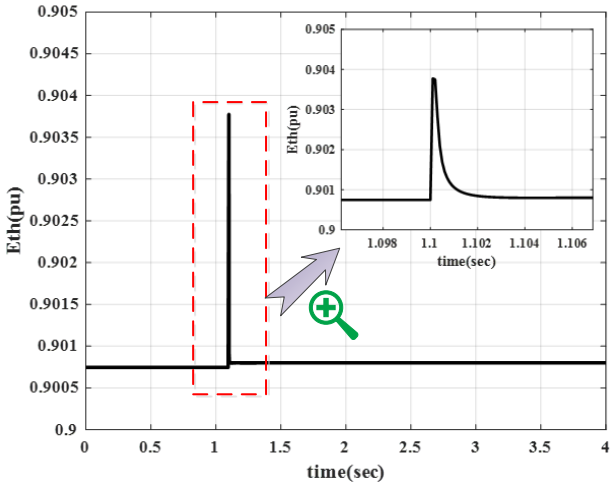

Fig. 8 The Thévenin voltage at the generator terminal bus.

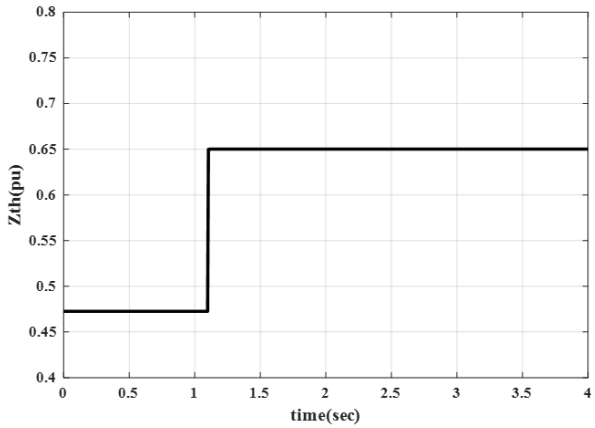

Fig. 9 The Thévenin impedance of network at the generator terminal bus.

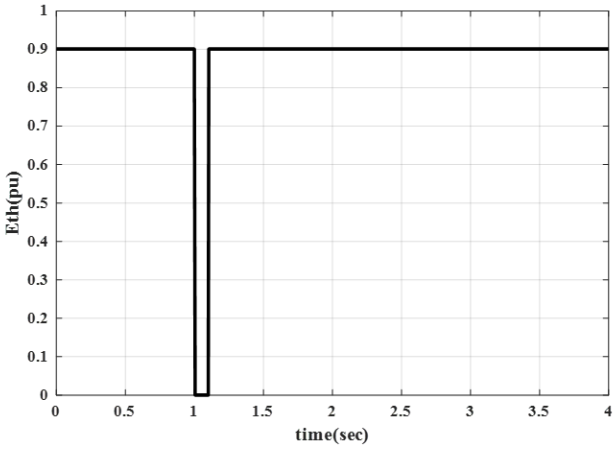

Fig. 10 The Thévenin voltage of network at the generator terminal bus.

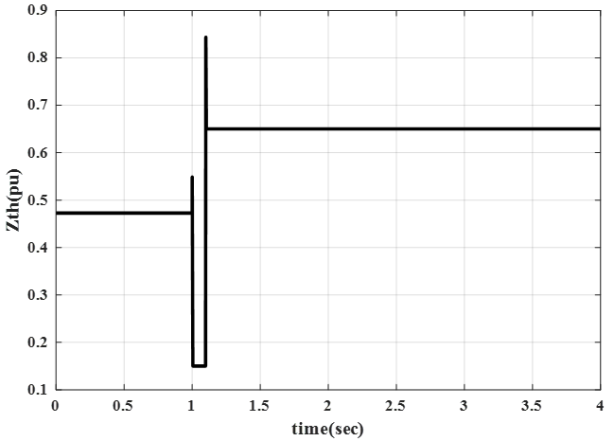

Fig. 11 The Thévenin impedance of network at the generator terminal bus.

Case 2: Line 2 is disconnected at t = 1.1 s after a three-phase fault at t = 1 s in point F

The three-phase fault scenario discussed in this section is occurred in the absence of STATCOM and the voltage and current phasor was sampled to the TE estimation. The sampling time step and initialization was set as case 1. The variation of the Thévenin voltage

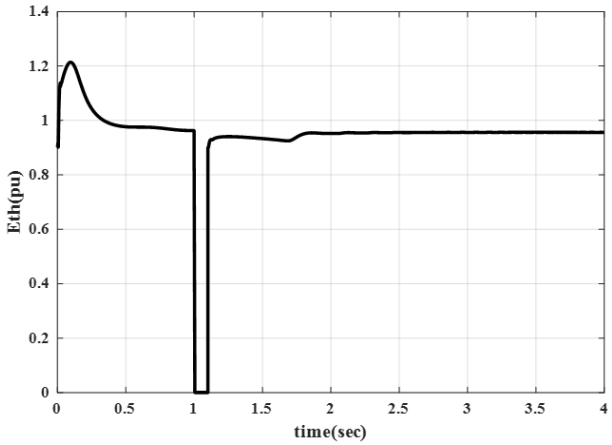

Fig. 12 The Thévenin voltage of network at the generator terminal bus in the presence of STATCOM.

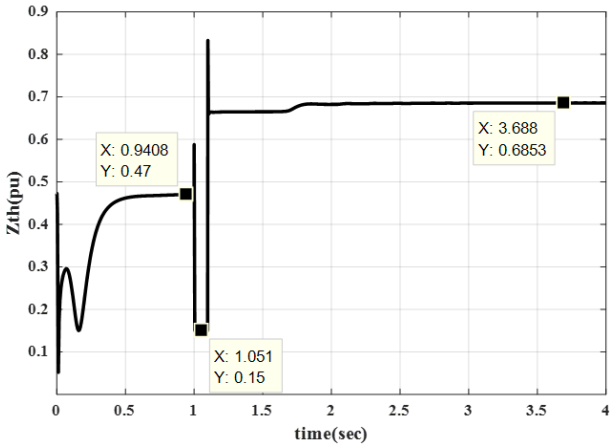

Fig. 13 The Thévenin impedance of network at the generator terminal bus in the presence of STATCOM.

and impedance are shown in Figs. 10 and 11, respectively. Similar to Case 1, the Thévenin voltage is identical before the fault and after the line is opened. That is equal to zero during fault. Moreover, the impedance is equal to 0.47 before the fault and it is equal 0.65 after the line is opened. During fault, the impedance is equal 0.15 pu that it is equal the impedance of step up transformer.

Case 3: Line 2 is disconnected at t = 1.1 s after a three-phase fault at the point F with a STATCOM connected to bus HT

In the third case the effect of STATCOM on the TE estimation has been examined. This case is similar to case 2 with a STATCOM connected to the bus HT. the simulation condition and TE estimator parameters are set similar to case 1. The results of this simulation are shown in Figs. 12 and 13. It is clear that dynamical behaviour of STATCOM cause the Thévenin voltage and impedance to be changed compared with case 2. In the steady state after disconnecting the line 2, the TE in the presence of STATCOM is equal to (14):

$$\theta_{SS} = \begin{bmatrix} E_{th} \\ Z_{th} \end{bmatrix} = \begin{bmatrix} 0.956\angle -0.126° \\ 0.6853\angle 89.78° \end{bmatrix} \tag{14}$$

6.2 The Effect of Measurements Errors on the Accuracy of Estimation

Case 2 in the previous sub section is used to evaluate the effect of measurement errors. The accuracy of measuring instruments affects the algorithm's output, slightly. To investigate this issue, random numbers with normal distribution are generated and summed with the measured voltage and current. The generation of random error numbers is done based on (15)-(17).

$$RN = a + (b - a) \times \text{rand} \tag{15}$$

$$a_v = -\frac{E_p}{100}\left|V^{measur}\right|, b_v = \frac{E_p}{100}\left|V^{measur}\right| \tag{16}$$

$$a_i = -\frac{E_p}{100}\left|I^{measur}\right|, b_i = \frac{E_p}{100}\left|I^{measur}\right| \tag{17}$$

In (15) 'rand' is a function that produces a random number in the interval 0 and 1 and *RN* is a random number in the specified range [*a* , *b*]. In (16) and (17), E_p is the error percentage and a_v, a_i, b_v, and b_i are the upper and lower limit of voltage and current errors, respectively. Moreover, V^{measur} and I^{measur} are the measured values of voltage and current. Thevenin equivalent with respect to the sampling error percentage of 0, 1, 5, and 10 percent are shown in Figs.14 and 15, respectively. It is clear that for E_p = 1 and E_p = 5, estimation is done properly and the estimation error is less than 5 percent in the all above error percentage.

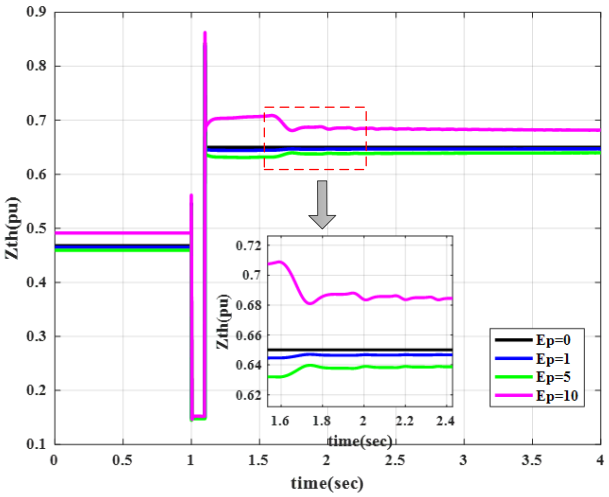

Fig. 14 The Thévenin impedance estimation by considering measurement errors.

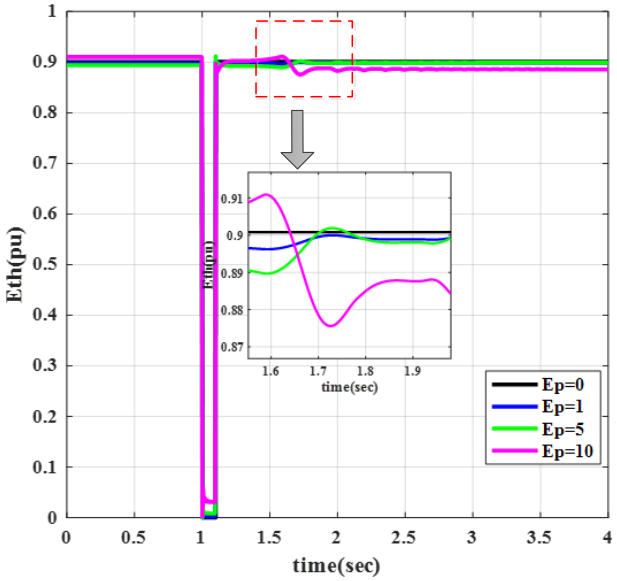

Fig. 15 The Thévenin voltage estimation by considering measurement errors.

6.3 The Modified Impedance Trajectory Based on TE

In this section, the impedance trajectory correction is performed based on (8) described in Section 4. The fault scenario similar to case 3 in the previous subsection is implemented here to compare the result with [34].

In (8) Z_1 is sub transient direct axis impedance of generator and is set 0.3 pu and Z_2^{new} is the network side Thévenin impedance in the absence of STATCOM after clearing fault that is equal to 0.65 pu. The Thévenin voltage shown in Fig. 12 is used instead of $\tilde{E}_{th}^{e}$ in (8) and finally, the internal voltage $\tilde{E}_1$ is calculated based on direct approach, discussed in [34]. The modified impedance trajectory with TE approach and the analytical approach discussed in [34] are compared together in Fig. 16. Moreover, the measured impedance trajectory is compared with two modification approaches in this figure. It is clear, that the proposed approach based on TE, corrects the path as in the previous method in [34]. The characteristic entry times (t_{en}), crossing times with imaginary axis ($t_{\delta=180}$ and the times out of characteristic (t_{out}) are listed in Table 1. It can be seen that the detection and operation times ($t_{\delta=180}$ and t_{out}, respectively) of two modification approach are almost identical. The 'ND' stands for Not Detected in this table.

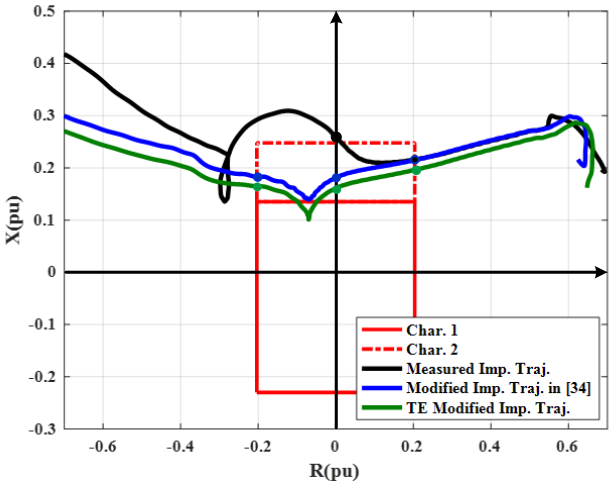

Fig. 16 The compare of modified trajectory with two strategies.

Fig. 17 shows the TE-based modified impedance trajectory during OOS condition. It is clear that the proposed approach corrects the impedance trajectory for all oscillation time of power swing. This is important when the relay is set to operate in the n'th oscillation of power swing.

The impact of fault location is investigated by changing the location of the fault into the middle and end of the second transmission line. The results of this study about fault location impact are summarized in Table 2. In this table, F1, F2 and F3 represent the fault location at the first, middle and end of transmission line, respectively. The 'MI' stands for 'Measured Impedance' in Table 2.

As the fault moves away from the generator, the critical clearing time (t_c) increases and to create OOS conditions, the fault needs to last longer in the network. To create OOS conditions, the fault is occurred at any fault location and last 0.03 sec longer than corresponding critical clearing time. The column t_{Clear} represents the fault clearing time corresponding to any fault location. Based on the detection time in Table 2, it is clear that the TE-based modified algorithm and the modification discussed in [34] have almost same results. The measured/modified impedance trajectories after fault at the middle and end of transmission line are shown in Figs. 18 and 19, respectively.

The performance of proposed method in the stable power swing has examined by decreasing fault clearing time to 1.08 s. Fig. 20 shows the modified impedance trajectory during stable condition of rotor angle. In the stable power swing both proposed approach and the analytical approach presented in [34] have almost identical results. In this condition, the impedance trajectory does not enter into the OOS characteristic and it converges to a point outside of the characteristic with damping the rotor angle oscillations.

Table 1 The entry and exit time of measured/ modified impedance trajectory.

	t_{en} [sec]	$t_{\delta=180}$ [sec]	t_{out} [sec]
Measured impedance	1.49	1.635	ND
Modified impedance in [34]	1.49	1.622	1.702
TE Modified impedance	1.49	1.622	1.70

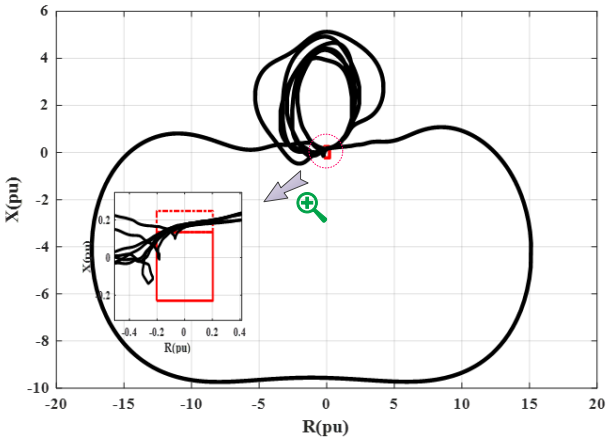

Fig. 17 The TE modified impedance trajectory during OOS condition.

Table 2 The impact of fault location on the performance of TE-based modified approach.

Fault location	Detection approach	t_c [sec]	t_{Clear} [sec]	$t_{\delta=180}$ [sec]	t_{out} [sec]	Detection time [sec]
F1	MI	1.082	1.112	1.635	-	ND
	[34]			1.622	1.702	0.702
	TE			1.622	1.7	0.7
F2	MI	1.215	1.245	1.675	1.78	0.78
	[34]			1.65	1.758	0.758
	TE			1.66	1.74	0.74
F3	MI	1.325	1.355	2.22	-	ND
	[34]			2.18	2.29	1.29
	TE			2.185	2.28	1.28

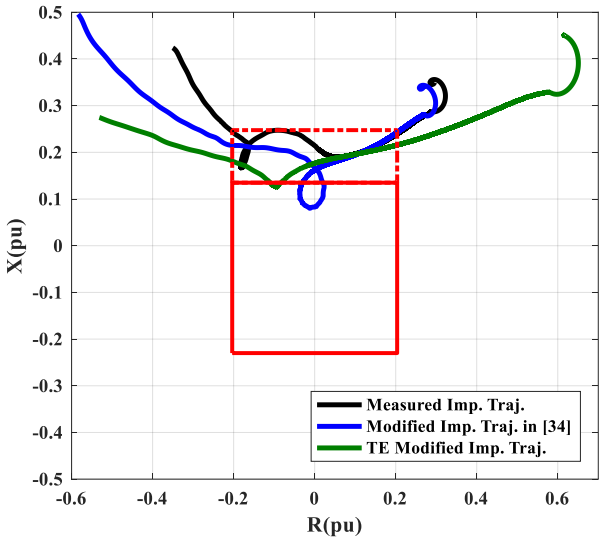

Fig. 18 Impedance trajectory after a the fault at the middle of transmission line (F2).

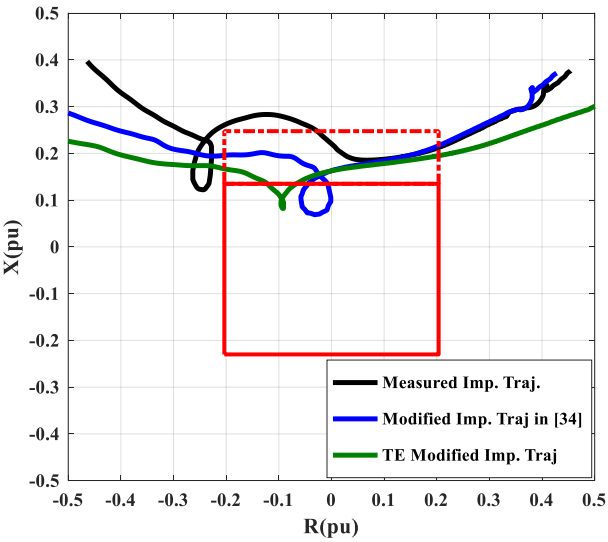

Fig. 19 Impedance trajectory after the fault at the end of transmission line (F3).

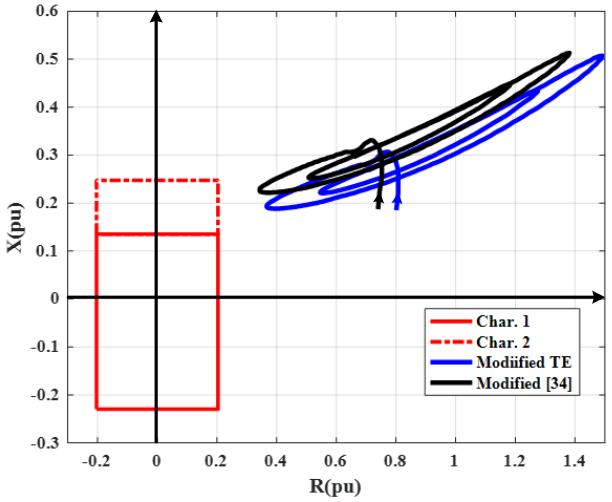

Fig. 20 The modified impedance trajectory in the stable power swing.

7 Conclusion

In this paper, a novel approach based on Thévenin tracing is presented to modify impedance trajectory of conventional impedance-based OOS protection. An approach based on recursive least square (RLS) is used to estimate the network Thévenin equivalent as on-line. Moreover, an OOS protection function is developed according to online network Thévenin equivalent parameters to correct the measured impedance trajectory. The main feature of this method is the use of local voltage and current measurements for Thévenin equivalent estimation and OOS protection. The performance of proposed method is investigated by simulation of synchronous generator OOS protection function in the presence of STATCOM. The simulation results of TE estimator show that the proposed approach estimates the network TE exactly. Also, another simulation indicates that the STATCOM changes the measured impedance path and it can cause misdiagnosis of OOS relay. Finally, the results show that the proposed approach corrects the impedance path and improves the accuracy of the OOS function when the STATCOM is used in system.

References

[1] P. Kundur, "Power system stability and control," New York: Mc-GrowHill, 1994.

[2] B. Alinezhad and H. K. Kargar, "Out-of-step protection based on equal area criterion," *IEEE Transasctions on Power Delivery*, Vol. 32, No. 2, pp. 968–977, Mar. 2017.

[3] B. Alinezhad and H. K. Kargar, "A novel out-of-step protection algorithm based on wide area measurement system," in *10th Power Systems Protection & Control Conference (PSPC)*, Tehran, Iran, 2016.

[4] A. Redfer, "A review of pole slipping protection," *IEE Colloquium on Generator Protection*, Newcastle, UK, pp. 6/1–6/9, 1996.

[5] P. M. Anderson, "Protective schemes for stability enhancement," in *Power system protection*. New York, IEEE Press, pp. 853–912, 1998.

[6] D. Reimert, "Loss of synchronism," in *Protective relaying for power generation systems*. New York, CRC Press Taylor & Francis Group, 2006.

[7] Y. Xue, T. Van Custem, and M. Ribbens-Pavella, "Extended equal area criterion justifications, generalizations, applications," *IEEE Transactions on Power Systems*, Vol. 4, No. 1, pp. 44–52, Feb. 1989.

[8] V. Centeno, A. Phadke, A. Edris, J. Benton, M. Gaudi, and G. Michel, "An adaptive out-of-step relay," *IEEE Transasctions on Power Delivery*, Vol. 12, No. 1, pp. 61–71, Jan. 1997.

[9] S. Paudyal, G. Ramakrishna, and M. S. Sachdev, "Application of equal area criterion conditions in the time domain for out-of-step protection," *IEEE Transasctions on Power Delivery*, Vol. 25, No. 2, pp. 600–609, Apr. 2010.

[10] S. Paudyal and R. Gokaraju, "Out-of-step protection for multi-machine power systems using local measurements," in *IEEE Eindhoven PowerTech*, Eindhoven, 2015.

[11] IEEE Power System Relaying Committee Working Group D6, "Power Swing and out-of-step considerations on transmission lines," Jun. 2005.

[12] E. Farantatos, G. J. Cokkinides, and A. P. Meliopoulos, "A predictive generator out-of-step protection and transient stability monitoring scheme enabled by a distributed dynamic state estimator," *IEEE Transasctions on Power Delivery*, Vol. 31, No. 4, pp. 1826–1835, Aug. 2016.

[13] T. S. Sidhu, R. K. Varma, P. K. Gangadharan, F. A. Albasri, and G. R. Ortiz, "Performance of distance relays on shunt-facts compensated transmission lines," *IEEE Transasctions on Power Delivery*, Vol. 20, No. 3, pp. 1837–1845, Jan. 2005.

[14] X. Zhou, H. Wang, R. K. Aggarwal, and P. Beaumont, "The impact of STATCOM on distance relay," in *15th PSCC*, Liege, pp. 22–26, Aug. 2005.

[15] X. Zhou, H. Wang, R. K. Aggarwal, and P. Beaumont, "Performance evaluation of a distance relay as applied to a transmission system with UPFC," *IEEE Transasctions on Power Delivery*, Vol. 21, No. 3, pp. 1137–1147, Jul. 2006.

[16] M. Khederzadeh and T. S. Sidhu, "Impact of TCSC on the protection of transmission lines," *IEEE Transasctions on Power Delivery*, Vol. 21, No. 1, pp. 80–87, Jan. 2006.

[17] F. A. Albasri, T. S. Sidhu, and R. K. Varma, "Performance comparison of distance protection schemes for shunt-FACTS compensated transmission lines," *IEEE Transasctions on Power Delivery*, Vol. 22, No. 4, pp. 2116–2125, Oct. 2007.

[18] M. Khederzadeh and A. Ghorbani, "STATCOM modeling impacts on performance evaluation of distance protection of transmission lines," *European Transaction on Electrical Power*, Vol. 21, No. 8, pp. 2063–2079, Nov. 2011.

[19] A. Ghorbani, "Comparing impact of STATCOM and SSSC on the performance of digital distance relay," *Journal of Power Electronics*, Vol. 11, No. 6, pp. 890–896, 2011.

[20] A. Ghorbani, B. Mozafari, and M. Khederzadeh, "Impact of SVC on the protection of transmission lines," *International Journal of Electrical Power and Energy Systems*, Vol. 42, No. 1, pp. 702–709, Nov. 2012.

[21] M. Khederzadeh and A. Ghorbani, "Impact of VSC-based multiline FACTS controllers on distance protection of transmission lines," *IEEE Transasctions on Power Delivery*, Vol. 27, No. 1, pp. 32–39, Jan. 2012.

[22] A. Ghorbani, B. Mozafari, S. Soleymani, and A. M. Ranjbar, "Operation of synchronous generator LOE protection in the presence of shunt FACTS," *Electric Power Systems Research*, Vol. 119, pp. 178–186, 2015

[23] M. Pazoki, Z. Moravej, M. Khederzadeh, N. K. C. Nair, "Effect of UPFC on protection of transmission lines with infeed current," *International Transactions on Electrical Energy Systems*, Vol. 26, No. 11. pp. 2385–2401, 2016.

[24] M. Elsamahy, S. O. Faried, and T. Sidhu, "Impact of midpoint STATCOM on generator loss of excitation protection," *IEEE Transasctions on Power Delivery*, Vol. 29, No. 2, pp. 724–732, Apr. 2014.

[25] A. Ghorbani, S. Soleymani, and B. Mozafari, "A PMU-based LOE protection of synchronous generator in the presence of GIPFC," *IEEE Transasctions on Power Delivery*, Vol. 31, No. 2, pp. 551–558, Apr. 2016.

[26] K. Raghavendra, S. P. Nangrani, and S. S. Bhat, "Modeling of Operation of loss of excitation relay in presence of shunt FACTS devices," in *6th International Conference on Power Systems*, pp. 1–6, 2016.

[27] H. Yaghobi, "A new adaptive impedance-based LOE protection of synchronous generator in the presence of STATCOM," *IEEE Transasctions on Power Delivery*, Vol. 32, No. 6, pp. 2489–2499, Dec. 2017.

[28] A. Esmaeilian, A. Ghaderi, M. Tasdighi, and A. Rouhani, "Evaluation and performance comparison of power swing detection algorithms in presence of series compensation on transmission lines," in *10th International Conference on Environment and Electrical Engineering (EEEIC)*, Rome, pp. 1–4, 2011.

[29] S. Jamali and H. Shateri, "Locus of apparent impedance of distance protection in the presence of SSSC," *International Transactions on Electrical Energy Systems*, Vol. 21, No. 1, 2011.

[30] P. Nayak, A. Pradhan, and P. Bajpai, "A fault detection technique for the series-compensated line during power swing", *IEEE Transasctions on Power Delivery*, Vol. 28, pp. 714–722, 2013.

[31] Z. Moravej, M. Pazoki, and M. Khederzadeh, "Impact of UPFC on power swing characteristic and distance relay behavior," *IEEE Transasctions on Power Delivery*, Vol. 29, No. 1, pp. 261–268, Feb. 2014.

[32] J. Khodaparast, M. Khederzadeh, F. F. D. Silva, and C. Leth Back, "Performance of power swing blocking methods in UPFC compensated line," *International Transactions on Electrical Energy Systems*, Vol. 27, No. 11, 2017.

[33] S. R. Hosseini, M. Karrari, and H. Askarian Abyane, "Performance evaluation of impedance-based synchronous generator out-of-step protection in the presence of unified power flow controller," *Electrical Power and Energy System*, Vol. 114, Jan. 2020.

[34] S. R. Hosseini, M. Karrari, and H. Askarian Abyane, "Impedance-based out-of-step protection of generator in the presence of STATCOM," *Iranian Journal of Electrical and Electronic Engineering*, Vol. 15, No. 4, Dec. 2019.

[35] *Multifunctional Machine Protection 7UM62 Manual*. 4.6 Ed. Siemens Co., pp. 165–174, 2010.

[36] J. P. Norton, "An introduction to identification," *Courier Corporation*, Apr. 2009.

S. R. Hosseini received the B.Sc. and M.Sc. degree in Electric Power Engineering from Zanjan University (Zanjan, Iran), Isfahan University of Technology (Isfahan, Iran) in 2006 and 2009, respectively. Currently, he is pursuing the Ph.D. degree. His research interests include power system protection, flexible AC transmission systems devices, and Power Generation. His current research work is in wide-area power system protection and control.

M. Karrari received the Ph.D. degree in Control Engineering from Sheffield University, Sheffield, U.K., in 1991. Since 1991, he has been with the Amirkabir University of Technology, Tehran, Iran. He is author or coauthor of more than 100 technical papers and two books: Power System Dynamics and Control, 2004, and System Identification, 2012, all in Persian. His main research interests are power system modeling, modeling and identification of dynamic systems, and large-scale and distributed systems.

H. Askarian Abyaneh (SM'09) was born in Abyaneh, Isfahan, Iran, on March 20, 1953. He received the B.Sc. and M.Sc. degrees, both in Iran, in 1976 and 1982, respectively. He also received another M.Sc. degree and the Ph.D. degree from the University of Manchester Institute of Science and Technology, Manchester, U.K., in 1985 and 1988, respectively, all in Electrical Power System Engineering. He published over 100 scientific papers in international journals and conferences. Currently, he is a Professor with the Department of Electrical Engineering, Amirkabir University of Technology, Tehran, Iran, working in the area of the relay protection and power quality.